

Simultaneous Operational AgI and Hygroscopic Flare Seeding in Texas: Rationale and Results

William L. Woodley
Woodley Weather Consultants
Littleton, Colorado

and

Daniel Rosenfeld
Hebrew University of Jerusalem
Jerusalem, Israel

Abstract A case study on 11 August 1996 involved simultaneous operational seeding of clouds to the W and SW of San Angelo, Texas, with hygroscopic flares at cloud base ($T = 16^{\circ}$) and with ejectable AgI flares near cloud top ($T = -8^{\circ}\text{C}$). Twenty-three hygroscopic flares were expended over 99 min while 95 AgI flares were expended over 96 min in the same area of clouds. The rationale for these dual seedings is discussed. This case was evaluated with San Angelo, Texas, NEXRAD radar data by calculating the lifetime properties of the seeded and non-seeded cells. This included the derivation of echo height vs. rainfall relationships. No cloud physics data were available. Although some of the seeded clouds produced heavy rainfall, there were a few unseeded clouds within range of the radar that produced comparable rainfall amounts. Thus, the data do not permit an unequivocal assessment of the effects of dual simultaneous hygroscopic and silver iodide seeding on this day.

1. INTRODUCTION

A case study on 11 August 1996 involved the simultaneous operational seeding of clouds to the W and SW of San Angelo with hygroscopic flares at cloud base ($T = 16^{\circ}\text{C}$) and with ejectable AgI flares near cloud top ($T = -8^{\circ}\text{C}$). This exploratory operational exercise in rain enhancement was predicated on the conceptual model guiding hygroscopic seeding experiments on deep clouds (Mather et al., 1997). According to the latest version of this model, hygroscopic flare seeding apparently increases rainfall by the following steps: 1) introduction of cloud condensation nuclei (CCN) at cloud base by burning hygroscopic flares, 2) preferential activation of the larger CCN from the flares, leading to a broadening of the cloud droplet distribution, 3) growth of the larger cloud droplets into raindrops by natural coalescence processes in clouds which could not otherwise have "grown" raindrops through warm-rain processes, 4) the transport of the raindrops into the supercooled portion of the cloud

where the raindrops freeze due to their larger size, 5) invigoration of the cloud due to the released latent heat and growth of the frozen drops to large graupel by accretion of the cloud water resident in the updraft, and 6) increased radar-estimated rainfall at cloud base and presumably more rainfall at the ground, when the enhanced water mass moves downward through the cloud.

Steps 4 and 5 in the conceptual model call for the natural freezing of the raindrops induced by the hygroscopic seeding and their growth as graupel by accreting the cloud water. Studies in Thailand (Sudhikoses et al., 1998) suggest clouds containing supercooled raindrops will glaciate nearly twice as fast as clouds without raindrops (e.g., 6 min vs. 10 min for the supercooled cloud water content to drop to 50% of its initial maximum value). This supports the step in the hygroscopic seeding conceptual model calling for the freezing of the raindrops induced by the hygroscopic seeding. If the clouds are seeded further with silver iodide (AgI), the glaciation

will be accelerated (Rosenfeld and Woodley, 1997; Sudhikoses et al., 1998). Because early freezing of supercooled raindrops to promote the formation and growth of graupel is a goal of the seeding of deep clouds, AgI seeding was superimposed on clouds seeded with hygroscopic flares on 11 August 1996 with the expectation the dual seeding would produce a recognizable seeding signature in the radar data.

The coupled seeding on 11 August 1996 was viewed at the time as a one-time event unless the seeding signature was so strong as to be unequivocally caused by the seeding. It may be the first time such dual seeding has been done in either a research or operational context. What happened is recounted here.

2. RESULTS

Both seeder aircraft were airborne before 1530 CDT. Cloud base was at 2.1 km at a temperature of 16°C. The PPI presentation at 2007 GMT (1507 CDT, i.e., CDT = GMT - 5hrs) from the San Angelo NEXRAD radar is shown in Figure 1. The distance between range rings is 50 km and the angular width between the depicted azimuths is 30°. The area of interest for operational seeding was a short line of broken echoes SE-SW of San Angelo between 45 and 70 km. The first hygroscopic flare was ignited at 1549 CDT 55 km from the radar, ranging between azimuths of 209° and 235° during the first 20min of base seeding. The first AgI flare was ejected at 1558 CDT 67km to the SSW of San Angelo. By 1607 CDT both aircraft were seeding in the same area as shown. The echo presentations at 2054 GMT (1554 CDT) and 2117 GMT (1617 CDT) are given in Figures 2 and 3. The new echo development about 75km to the W of the radar had not been seeded at this time.

The echoes continued to develop to the NW as they dissipated at the SE end of the broken line. The base and top seedings moved NW with the new echoes (Figures 4 and 5). The echo mass had become better organized by 2210 GMT (1710 CDT) under continuing base and top seeding (Figure 6). The last radar image was at 2216 GMT (1716 CDT) (Figure 7) but seeding continued at cloud base until 1728 CDT and at cloud top until 1734 CDT. The reason for the lapse in radar data is unknown. The echo mass continued strong in the area of seeding through at least 1740 CDT as assessed subjectively in real time by viewing the project radarscope. (The project radar data were not used quantitatively in this analysis.) By 1800 CDT the echoes were dissipating as they drifted to the W and SW, although there are no NEXRAD data for documentation purposes.

Twenty-three hygroscopic flares had been expended over 99 min while 95 AgI flares had been expended on 31 cloud passes over 96 min in the same area of clouds. This case was evaluated with the NEXRAD radar data by calculating the lifetime properties of the seeded and non-seeded cells until they merged with other echoes or dissipated. This is called the "short-track" analysis using the methods of Rosenfeld (1987). No cloud physics data are available for this case.

The summed rainfall for the period of seeding until the gap in the radar data is shown in Figure 8, where $Z = 300R^{1.5}$ was used to relate radar reflectivity (Z) to rainfall rate (R). Referring to the legend relating the color contours to rain depths, one can see the rainfall was heavy in the seeded area (i.e., azimuths between 210° and 260° at 60km to 90km from the radar). The rainfall was also heavy in cores elsewhere, so there does not appear to be anything unique about the area of seeding. The maximum radar-estimated rainfalls range up to 75mm at several

locations over the map. The rain depths are underestimated at the NW end of the treated line because of the truncation of the radar data. A rancher under the seeded clouds reported a maximum of 100mm on his ranch.

Plots of maximum echo heights (H_{max}) vs. maximum reflectivity (Z_{max}) and maximum echo heights vs. their total lifetime rain volumes are provided in Figures 9 and 10, respectively. The treated cells are identified as red dots. Clouds producing $< 100 \text{ m}^3$ of rain volume are plotted as $0.1 \times 10^3 \text{ m}^3$ on the logarithmic scale. Eight of the 20 tracked seeded cells were quite reflective and rain productive. There were a few unseeded echoes, however, that were just as strong, so one cannot determine whether and by how much the rainfall may have been enhanced by the simultaneous coupled seedings.

3. DISCUSSION AND CONCLUSIONS

Current studies underway by the authors in Texas and Thailand show unequivocally clouds with strong coalescence are the most rain-productive, especially if those clouds are supercooled. Such clouds will produce early freezing of the seeding-induced raindrops resulting in the formation of graupel which can grow in the invigorated updraft by accreting the resident cloud water. Thus, artificial seeding that imitates this natural process is likely to be successful in increasing the rainfall. Simultaneous use of hygroscopic agents at cloud base and AgI near the supercooled cloud tops was viewed as one possibility. The hygroscopic seeding would generate raindrops and the AgI would promote their early freezing.

It was this prospect that prompted the *exploratory dual operational seeding* on 11 August 1996. The test was highly successful operationally, but there is no

proof of the efficacy of the dual seeding. Although the seeded clouds organized into strong rain-productive masses, the seeding signature relative to the natural background is not strong enough to constitute proof the clouds reacted differently by virtue of the seeding.

Contributing to this uncertainty are two potential factors. First, the natural clouds on this day likely had some natural coalescence and raindrops. This would decrease the hygroscopic seeding signature relative to the non-seeded clouds of the day. Second, we were not able to bring to bear enough measurement firepower for the documentation of this case. Not having in-cloud microphysical measurements was a distinct disadvantage. There is just so much that can be done with case studies identified in the context of operational seeding.

It is the collective weight of the evidence over several research case studies in conjunction with randomized experimentation that will ultimately demonstrate the efficacy of cloud seeding. Cloud and mesoscale models, which simulate natural processes realistically, are vital also for the discernment of seeding effects. Although much can be learned from "piggybacking" with operational seeding programs in some instances, there is simply no substitute for a dedicated research program.

4. ACKNOWLEDGEMENTS

This research was supported by the Texas Resource Conservation Commission (TNRCC) under Agency Order No. 582-8-104352. Our special thanks to Mr. George Bomar of the TNRCC for his encouragement during the course of these studies.

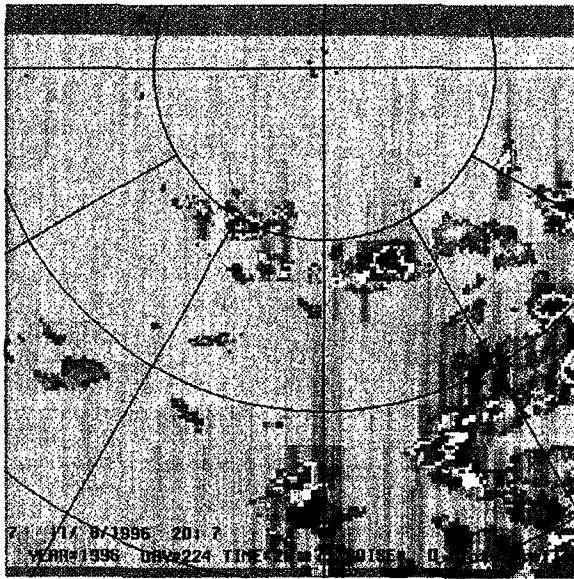


Figure 1. San Angelo PPI NEXRAD radar echo presentation at 2000 GMT on 11 August 1996. The color contours correspond to the following in dBZ: White > 60, light pink > 55, magenta > 50, orange > 45, gold > 40, yellow > 35, light green > 30, dark green > 25, light blue > 20, blue > 15, dark blue > 10, dark gray > 1, light gray > 0.

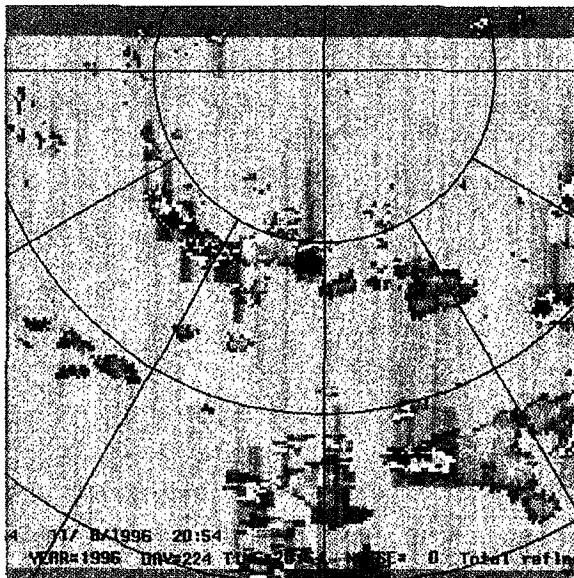


Figure 2. As in Figure 1 but for 2054 GMT.

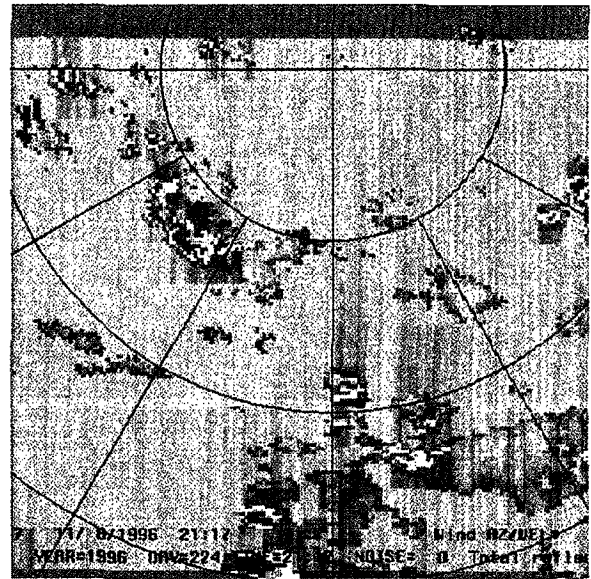


Figure 3. As in Figure 1 but for 2117 GMT

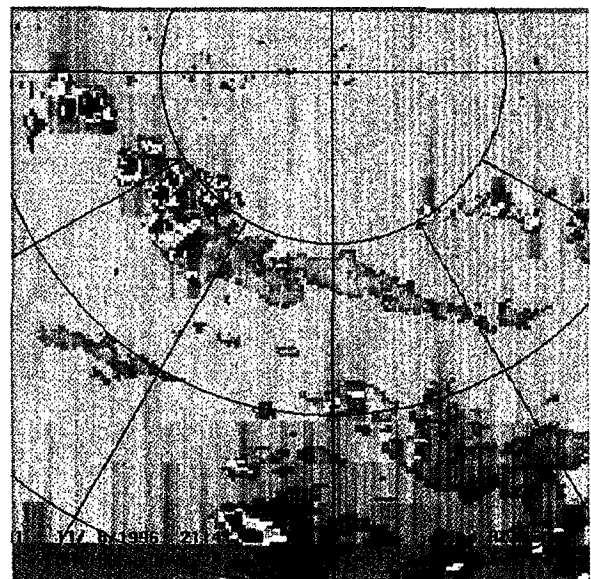


Figure 4. As in Figure 1 but for 2141 GMT.

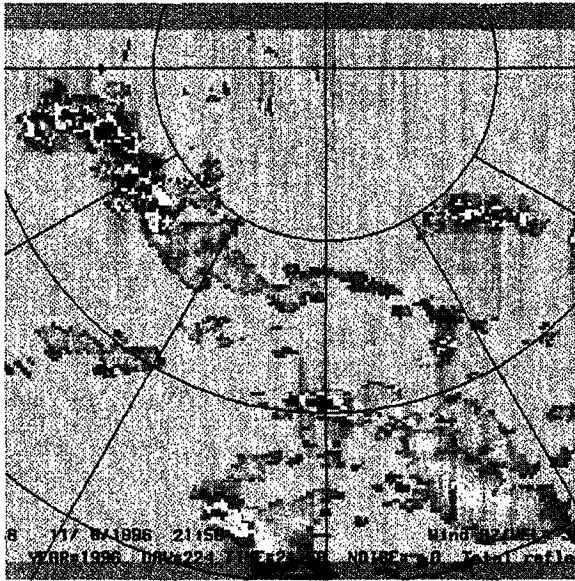


Figure 5. As in Figure 1 but for 2158 GMT.

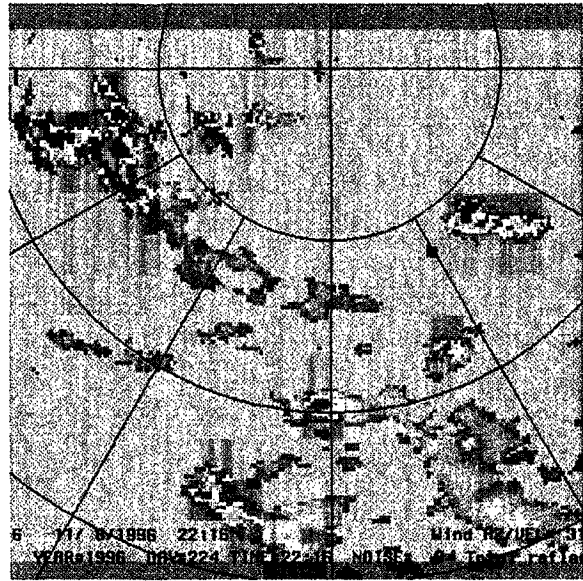


Figure 6. As in Figure 1 but for 2210 GMT.

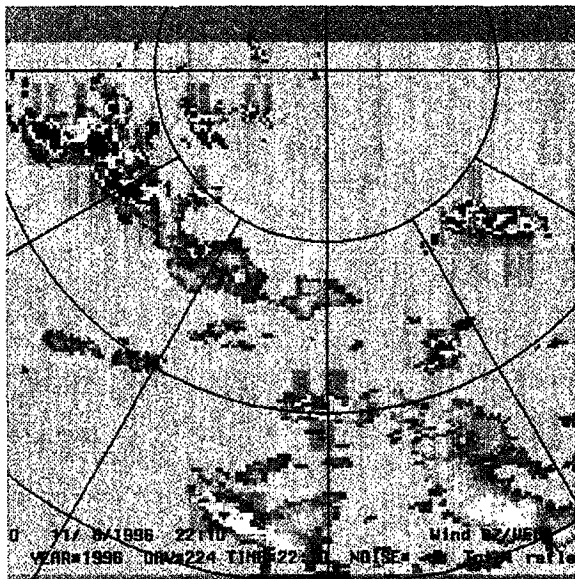


Figure 5. As in Figure 1 but for 2158 GMT.

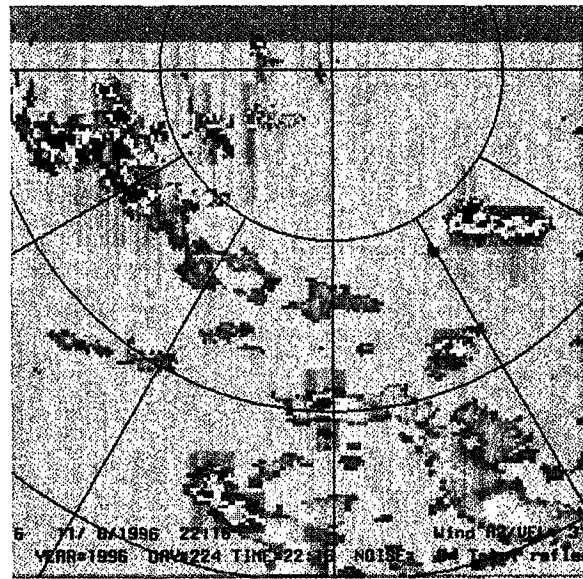


Figure 7. As in Figure 1 but for 2216 GMT. There are no radar data after this time.

5. REFERENCES

Mather, G.K., D.E. Terblanche, F.E. Steffens and L. Fletcher, 1997: Results of the South African cloud seeding experiments using hygroscopic flares. *J. Appl. Meteor.*, 36, 1433-1447.

Rosenfeld, D., 1987: Objective method for tracking and analysis of convective cells as seen by radar. *J. Atmos. Sci.*, **4**, 422-434.

Rosenfeld, D., and W.L. Woodley, 1997: Cloud microphysical observations of relevance to the Texas cold-cloud conceptual seeding model. *J. Wea. Mod.*, **29**, 56-69.

Sudhikoses, P., W. Sukarnjanaset, N. Tantipubthong, W.L. Woodley, and D. Rosenfeld, 1998: Cold-cloud microphysical observations in seeded and non-seeded Thai clouds. Preprints, AMS Conf. On Cloud Physics 17-21 August 1998, Seattle, Washington.

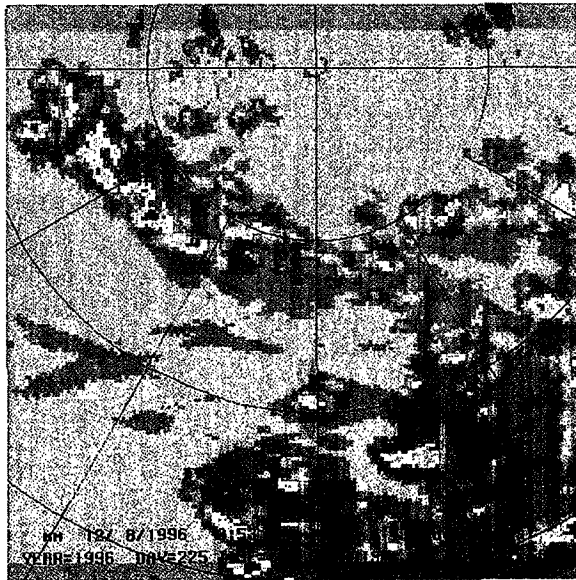


Figure 8. A summation of the radar-estimated rainfalls for the convective cells during the seeding period as discussed in the text. The color contours correspond to the following in mm: White > 150, light pink > 100, magenta > 75, orange > 50, gold > 30, yellow > 20, light green > 15, dark green > 10, light blue > 6, blue > 4, dark blue > 2, dark gray > 1, light gray > 0.

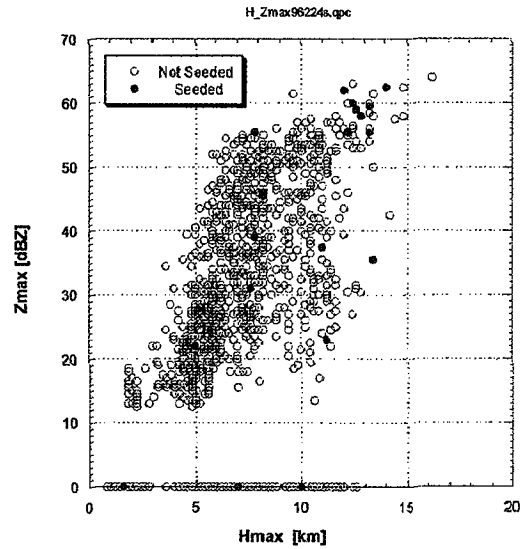


Figure 9. Scatter plot of the maximum height of the echoes (Hmax) vs. their maximum radar reflectivity (Zmax) for the seeded and non-seeded cells.

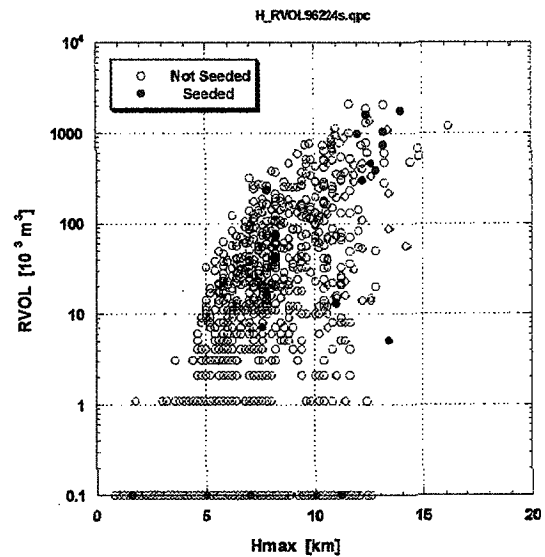


Figure 10. Scatter plot of the maximum height of the echoes (Hmax) vs. their total lifetime rain volumes (RVOL) for the seeded and non-seeded cells.